

Evaluation of tsunami fragility curves for building damage level allocation

Luis MOYA*, Erick MAS*, Shunichi KOSHIMURA*

1. Abstract

This paper discusses the applicability of tsunami fragility curves to estimate the damage of buildings due to tsunami. Tsunami fragility curves have been developed empirically out of the damage data obtained from large scale tsunami disasters (Koshimura et al., 2009; Mas et al., 2012a; Suppasri et al., 2011, 2013). Fragility curves can provide an overall idea of the impact of a tsunami event, however, for disaster mitigation purposes a desired application for these curves is the assessment of possible future damage due to tsunami. Thus, this report aims on evaluating the applicability of tsunami fragility curves for building damage estimation. Our hypothesis is that a building damage estimation due to tsunami performed with fragility curves developed in the same location and urban characteristics (i.e. building type, layout, topography, etc.) should provide a high accuracy. This is expected since the data (event and buildings) used to develop the fragility curve contains the sample use for the evaluation. However, a high accuracy in this descriptive and overfitting exercise does not ensure a high accuracy on the predictive exercise. In contrast, if a low accuracy is found in here, is very likely that the same fragility curve applied in a different area will present low accuracy. This report is organized as follows: first, an introduction and background of fragility curves theory and development is briefly explained. In addition, its application to tsunami damage estimation

in previous literature is reported. Next, we will present the methodology used in this report to test the applicability of fragility curves for tsunami damage estimation. Finally, results and discussion on the limitations and accuracy of tsunami fragility curves is presented. We conclude in this report that tsunami fragility curves present low accuracy when applied and evaluated at micro scale levels of building damage estimation. However, the macro scale evaluation of tsunami is, as expected, fairly acceptable. A remaining gap is the effective use of tsunami fragility curves when building-by-building damage estimation is required and the discussion on the transferability of these curves to other localities, even when assessing damage at the macro scale level.

2. Background

2.1. Developing fragility curves

Building damage estimation was first developed for earthquake events. Most of the approaches are made in a probabilistic context. Risk analysis uses scenario events. The majority of seismic risk studies aimed to estimate the building damage as a percentage of buildings survived and buildings at different damage states. Seismic risk analysis proved to be crucial for decision process. A fragility curve represents the probability that an asset (i.e., buildings for our purpose) under a given level of the engineering demand parameter (EDP) reaches or exceeds certain level of damage. In general, for risk analysis, fragility curves are expressed as a logarithmic cumulative distribution function:

* Laboratory of Remote Sensing and Geoinformatics for Disaster Management, IRIDeS, Tohoku University

$$F_d(edp) = P[D \geq d | EDP = edp]$$

$$F_d(edp) = \Phi\left(\frac{\ln(edp/x_m)}{\beta}\right) \quad (1)$$

Where Φ refers to the normal cumulative distribution function, x_m denotes the mean value of the distribution, β is the logarithmic standard deviation, edp denotes a specific value of EDP , and d a specific damage state.

Koshimura et al. (2009) developed fragility functions from a tsunami inundation numerical model and survey data of the 2004 Sumatra-Andaman earthquake tsunami. Different tsunami features such as inundation depth, current velocity and hydrodynamic force were employed in their study. Two level of damage were used: destroyed and survived levels. Mas et al. (2012a) used the inundation depth values from post-tsunami field survey data of the 2010 Chile earthquake and building damage inventory from satellite imagery and developed a tsunami fragility function for the southwestern Pacific country of Chile. This study used two level of damage as well. On the other hand, Suppasri et al. (2013) used a large and very detailed building damage dataset from the 2011 Great East Japan Tsunami and developed a set of fragility curves to extract seven damage states: no damage, minor damage, moderate damage, major damage, complete damage, collapsed and washed away.

2.2. Damage estimation

In this study, damage is understood as the consequence of a disaster event (more specifically, a tsunami). As mentioned previously, damage estimation is mostly expressed as a probability and often used for loss estimation. Here, the damage estimation is expressed in macro scale. However, a number of methods that require a realistic estimation at individual/micro-scale level have rose in recent years. For instance, a discipline that has emerged with the widespread fast computation is agent-based modeling (ABM). ABM is a bottom-up

approach in which each agent or individual part of a system, under particular rules, according to their role in the system, is modeled as an autonomous decision making entity (Mas et al., 2015). Mas et al. (2012b) identified bottlenecks and congested streets during the 2011 Great East Japan Earthquake based on an evacuation simulation using ABM. Das and Hanaoka (2014) used ABM for allocating resources in various zones after a large scale disaster.

2.3. Application of fragility curves for damage estimation

Tsunami damage estimation based on fragility curves has been used widely. Adriano et al. (2014) used the fragility curves proposed by Suppasri et al. (2013) to estimate the fraction of damaged buildings for each damage level and presented scenarios of earthquake and tsunami damage mapping in Callao region, Peru. Rehman and Cho (2016) used the same set of fragility curves to perform fragility analysis for buildings vulnerable to flooding by tsunamis in the Imwon Port in Korea. Wiebe and Cox (2014) estimated buildings damage and economic loss for different synthetic tsunami events in Seaside, Oregon, USA, using the same set of fragility curves as well. As noticed, several damage estimations have been performed using the set of fragility curves constructed in Japan. However, up to now its performance in terms of transferability has been not evaluated.

3. Methodology

As pointed out, building damage estimation from risk analysis is usually provided as a ratio of the total buildings in a given area. However, further analysis using ABM requires the damage state for each building after a given disaster event. Common sense would suggest to perform a numerical simulation for each building. However, this option requires detailed information of the

mechanical and geometrical properties of each element of the structural system, which is often not available. In addition, the amount of buildings in a city, which is composed of hundreds of thousands of buildings, would require a significant amount of time and computational effort.

The method proposed here attempts to allocate a damage state to each geocoded building using fragility functions proposed in previous studies. The purpose here is to refine the scale until a building scale while keeping the percent of damage buildings in the overall scale at its minimum error. Thus, it will generate synthetic data for spatial units with different damage states for a given city that encompasses a set of buildings with different features. Buildings with same properties, such as construction material, number of floors and construction year, are grouped in subsets. Each subset is associated to its respective set of fragility curves. From the fragility curves, the distribution of damage states is extracted for each subset. Then, the synthetic data set is generated from a random generation sampling method using the distribution of damage states. The steps of the procedure are explained as follows:

(i) Group buildings with the same features. Those features taken into account have to include the features used in the preparation of the fragility curves. For instance, Suppasri et al. (2013) proposed different set of fragility curves for buildings with different materials (wooden, reinforced concrete, steel and masonry) and different number of floors (1, 2 and greater than 3). Figure 1 shows the fragility curves for wooden buildings with two stories, and Table 1 shows the necessary parameters to create them (Suppasri et al., 2013). The set of fragility functions clearly delimits the region of each damage state. The description of the damage states is provided in Table 2.

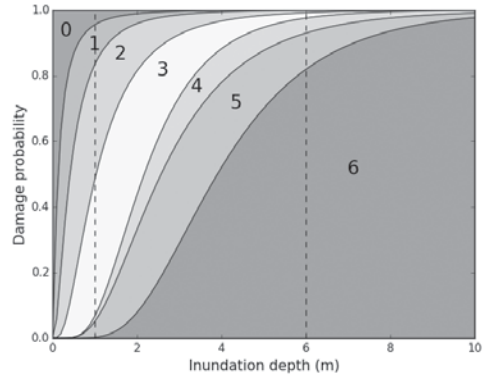


Figure 1: Tsunami fragility curves from Suppasri et al. (2013) or six damage states.

Table 1: Parameters of tsunami fragility functions used in this study

Material	x_m	β
W-2: damage level 1	-2.0080	1.1873
W-2: damage level 2	-0.8747	0.9053
W-2: damage level 3	0.0350	0.7387
W-2: damage level 4	0.7770	0.5153
W-2: damage level 5	0.9461	0.5744
W-2: damage level 6	1.3633	0.4710

Table 2: Damage state levels and their description

D	Description
0	No presence of damage
1	There is no significant structural or non-structural damage, possibly only minor flooding
2	Slight damage to non-structural components
3	Heavy damage to some walls but no damage in columns
4	Heavy damage to several walls and some columns
5	Destructive damage to walls (more than half of wall density) and several columns (bends or destroyed)
6	Washed away, only foundation remained, total overturned

(ii) Extract the EDP for each building. Several EDP has been used for tsunami building damage. Inundation depth, current velocity, hydrostatic force, hydrodynamic force and debris impact are such examples. However, the most common EDP is inundation depth because of its easy access.

(iii) Calculate the probability of the damage states for each building from the fragility function using the following equations:

$$\begin{aligned}
 P[D = d | EDP = edp] &= 1 - F_1(edp), & d = 0 \\
 &= F_d(edp) - F_{d+1}(edp), & 1 \leq d < N \\
 &= F_d(edp), & d = N
 \end{aligned}
 \tag{2}$$

where N denotes the number of possible damage states, in addition to non-damage state ($d = 0$). Figure 2 shows the damage probabilities for two wooden buildings of two stories. The first building has an EDP of 1m of inundation depth (thin bars) and the second has 6 m as EDP (thick bars). The probabilities were calculated using the set of fragility curves shown in Figure 1. It is observed that the first building is more likely to experience damage states of level 2 or 3, while the second building is more likely to experience damage level 6. An alternative interpretation is that the probability of damage states, such as the shown in Figure 2, represents the distribution of damage states for buildings with same features and same EDP.

(iv) Estimate the damage state using a random sampling technique, where the random sample is calculated using the probability distribution from (2). For instance, Figure 3 shows the histogram of three set of samples generated randomly using the distribution for wooden buildings of two stories with EDP of 1 m. The sets contain different number of samples. The sample A histogram was calculated from 10 samples, the sample B histogram with 100 samples and the sample C histogram with 1000 samples. The probability calculated from (2) is also shown as a cross marks. It is observed that the accuracy increases when the number of samples increases as well. In other words, the random sampling keeps the distribution in a large scale.

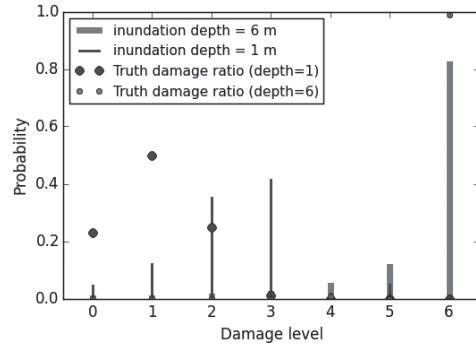


Figure 2: Damage probabilities for two wooden buildings of two stories

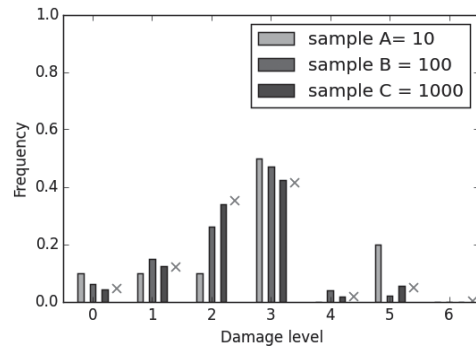


Figure 3: Histogram of synthetic data of damaged buildings (bars) and probabilities of damage for each damage state (cross marks)

4. Experimental result and analysis

To demonstrate the performance of the allocation method, the building damage produced in the bay of Sendai city after the 2011 Mw 9.0 Tohoku earthquake (hereafter The Tohoku earthquake) is used. The Tohoku earthquake is one of the biggest earthquake in the world that was well recorded. It struck beneath the Pacific Ocean off the coast of northeastern Japan and generated a big tsunami that affected 850 km long swath of the coast of Japan. Buildings placed in the East coast of Japan were significantly affected by the tsunami. Figure 4 shows the inundated area of the coast of Sendai city and the spatial distribution of damaged buildings. The number of affected buildings used in this study,

Table 3: Comparison between the total amount of damaged buildings surveyed by MLIT and that obtained from the simulation

D	0	1	2	3	4	5	6
MLIT	662	897	1978	1031	539	656	2925
Simulated	225	393	914	1506	880	1584	3186
error (%)	-66	-56	-53	+46	+63	+140	+9

according to the Ministry of Land, Infrastructure and Transportation of Japan (MLIT), is shown in Table 3.

The fragility curves proposed by Suppasri et al. (2013) are used for the allocation of damaged buildings. It is worth mentioning that (2) produced negative values for inundation depths close to zero, which is meaningless. For those cases the probability of damage was set to zero, as suggested by Porter et al. (2007). The inundation depth is provided by the MLIT and it ranges between 0 and 21.8 m in the coast of Sendai. This study focuses only on those buildings that has complete information (i.e., the construction material, and the number of stories), thus some surveyed buildings were discarded. Figure 5 shows the synthetic building damage distribution obtained from allocation procedure. The result, from an overall perspective seems consistent comparing with the truth data, with bundle buildings with damage level 5 and 6 near the bay, and lower damage stages on buildings located far from the coast. However, a closer look of areas such as the shown in Figure 5b and 5c indicates that the allocation produce an overestimation of the damage states. Figure 6 shows the confusion matrix obtained from a comparison of the synthetic damage distribution of buildings and the truth damage distribution surveyed by the MLIT. It is observed that the values of the upper triangular area are mostly greater than the values located in the lower triangular. Thus, it confirms that the allocation is producing an overestimated scenario. Table 3 shows the total amount of

estimated damaged buildings per damage state.

Furthermore, the allocation procedure was performed a hundred times and it was observed a steady behavior. Figure 7 shows the correlation coefficient (r) and the overall accuracy (OA) calculated between the synthetic and the truth building damage for each simulation, which are expressed as follows:

$$OA = \frac{\sum_{j=1}^6 M_{jj}}{T} \quad (3)$$

$$r = \frac{T \sum_{i=1}^T s_i t_i - \sum_{i=1}^T s_i \sum_{i=1}^T t_i}{\sqrt{\left(T \sum_{i=1}^T s_i^2 - \left(\sum_{i=1}^T s_i\right)^2\right) \left(T \sum_{i=1}^T t_i^2 - \left(\sum_{i=1}^T t_i\right)^2\right)}} \quad (4)$$

where M_{jj} is the amount of buildings whose predicted damage level coincide with the truth damage (i.e., the diagonal values of the matrix shown in Figure 6), T is the total number of buildings, s_i and t_i are the simulated and the truth damage level for building i , respectively. A value of r close to 1 indicates a good correlation between the synthetic and the truth data, while a zero value indicates no correlation. The r calculated from the simulations is fluctuating around 0.57, which shows a low correlation. The overall accuracy is calculated as the total amount of buildings that were well classified (i.e., the values located in the diagonal of the confusion matrix) divided by the total of buildings. The overall accuracy is fluctuating around 30%. The damage ratio for each damage state is also evaluated, Figure 8 depicts a comparison of the damage ratio between the synthetic (solid line) and the truth damage buildings (dashed line). The comparison shows that damage ratio for levels 0, 1 and 2 is underestimated. On the contrary, damage ratio for levels 3–6 are overestimated. The largest difference between synthetic and truth damage ratio is observed in damage state 2 with 12%.

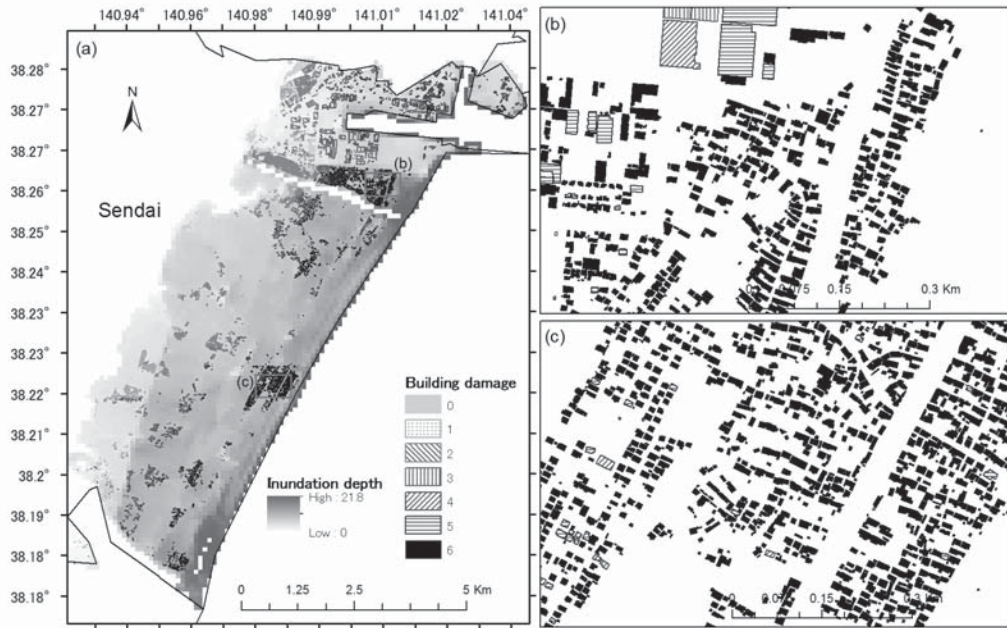


Figure 4: Damage in Sendai city due to the 2011 Great East Japan Earthquake and Tsunami according to the MLIT

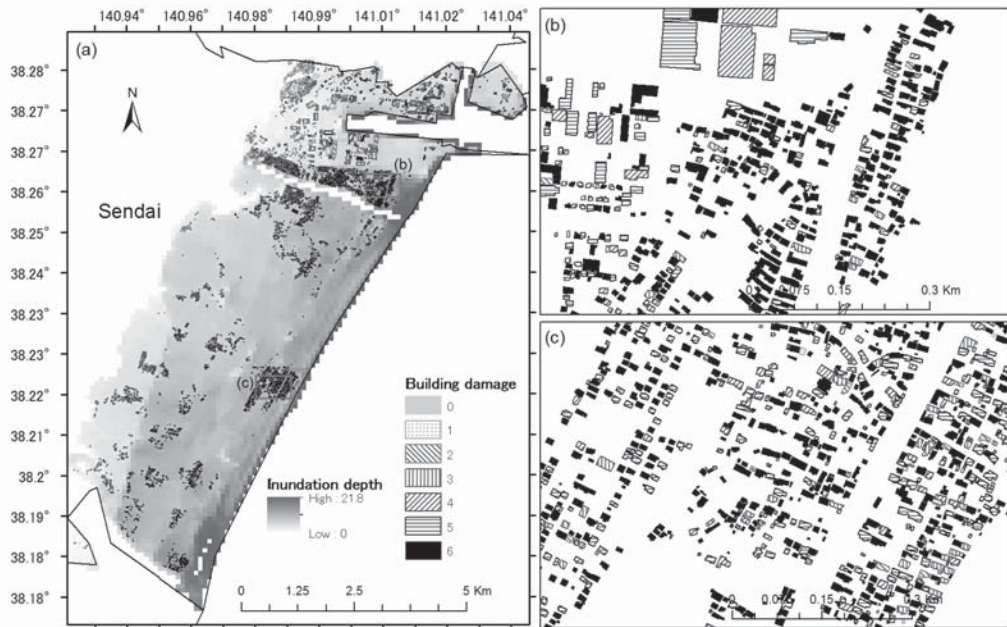


Figure 5: Synthetic building damage distribution obtained from allocation procedure

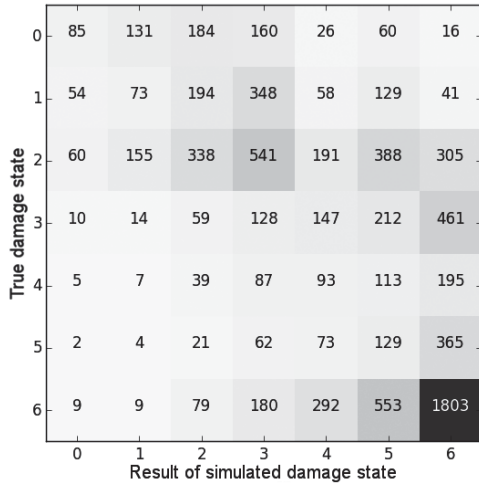


Figure 6: Confusion matrix of a damage scenarion

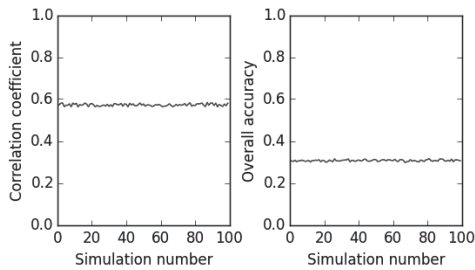


Figure 7: Correlation coefficient (left) and overall accuracy (right) calculated for each simulation

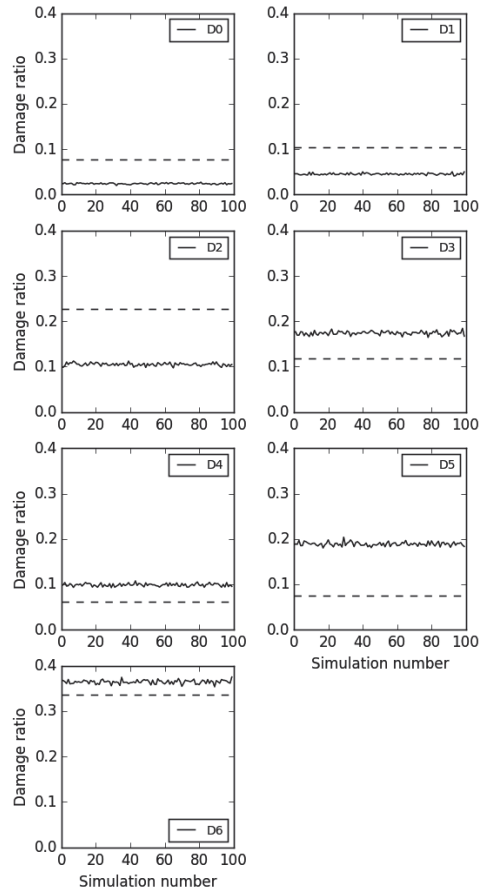


Figure 8: Simulated damage ratio

5. Discussion and Conclusions

This paper presents the allocation of damage states to geocoded buildings using fragility functions. A random sampling approach specifying the distribution obtained from the fragility curves is used. The procedure is tested for the building damage after the 2011 Mw 9.0 Tohoku earthquake over the coast of Sendai city. In general, the result shows an overestimation of the damage states 3–6 and an underestimation of damage states 0–2. Therefore the synthetic distribution of damage on buildings from this approach is conservative. We believe this consideration is crucial when a micro scale

damage estimation is required.

A comparison in a microscale between the truth damage distribution and that simulated (i.e., the overall accuracy and the correlation coefficient) shows low level of accuracy, which was expected considering the random allocating approach. Conversely, a high agreement was expected in the aggregate amount of damage; that is, the total amount of buildings per damage level (Recall that the random sampling was performed using a distribution calculated from the fragility curves). However, there are still some discrepancies observed in the estimation of total amount of damaged buildings (See Table 3 and Figure 8). Therefore, a closer look on the truth data was

necessary. Figure 2 shows the truth damage ratios for wooden house of two stories under two levels of inundation: 1 m (sample C) and 6 m (cross marks), within Sendai city. Besides, the damage ratios obtained from the fragility curves are also included in Figure 2 as thin and thick bars for inundations of 1 m and 6 m, respectively. A significant difference is observed between both damage ratios. It is worth to note the fragility curves used here were constructed from the whole tsunami affected areas, which covered seven provinces: Hokkaido, Aomori, Iwate, Miyagi, Fukushima, Ibaraki and Chiba (Suppasri et al., 2013). These results show, that two different levels of aggregation (Japan seven prefectures versus Sendai coast) are not consistent and the direct application of fragility curves might be comparatively more reliable at the macro scale assessment. This observation remarks that the use of fragility curves to other areas can produce larger errors than the ones observed here, and thus should be use carefully when trying to predict damage.

Acknowledgments

This research is supported by the Japan Science and Technology Agency (JST) through the SICORP project Increasing Urban Resilience to Large Scale Disaster: The Development of a Dynamic Integrated Model for Disaster Management and Socio-Economic Analysis (DIM2SEA) and the support of the International Research Institute of Disaster Science (IRIDeS) at Tohoku University.

References

- Adriano, B., Mas, E., Koshimura, S., Estrada, M., and Jimenez, C. (2014). Scenarios of earthquake and tsunami damage probability in callao region, Peru using tsunami fragility functions. *Journal of Disaster Research*, 9(6):968–975.
- Das, R. and Hanaoka, S. (2014). An Agent-based Model for Resource Allocation During Relief Distribution. *Journal of Humanitarian Logistics and Supply Chain Management*, 4(2):265–285.
- Koshimura, S., Oie, T., Yanagisawa, H., Imamura, (2009). Developing Fragility Functions for Tsunami Damage Estimation Using Numerical Model and Post-Tsunami Data From Banda Aceh, Indonesia. *Coastal Engineering Journal*, 51(3):243–273.
- Mas, E., Koshimura, S., Imamura, F., Suppasri, A., Muhari, A., and Adriano, B.(2015). Recent Advances in Agent-Based Tsunami Evacuation Simulations:Case Studies in Indonesia, Thailand, Japan and Peru. *Pure and Applied Geophysics*, 172(12):3409–3424.
- Mas, E., Koshimura, S., Suppasri, A., Matsuoka, M., Matsuyama, M., Yoshii, T., Jimenez, C., Yamazaki, F., and Imamura, F. (2012a). Developing Tsunami fragility curves using remote sensing and survey data of the 2010 Chilean Tsunami in Dichato. *Natural Hazards and Earth System Science*, 12(8):2689–2697.
- Mas, E., Suppasri, A., Imamura, F., and Koshimura, S. (2012b). Agent-based simulation of the 2011 Great East Japan earthquake/tsunami evacuation: An integrated model of tsunami inundation and evacuation. *Journal of Natural Disaster*, 34(1):41–57.
- Porter, K., Kennedy, R., and Bachman, R. (2007). Creating fragility functions for performance-based earthquake engineering. *Earthquake Spectra*, 23(2):471–489.
- Rehman, K. and Cho, Y.-S. (2016). Building Damage Assessment Using Scenario Based Tsunami Numerical Analysis and Fragility Curves. *Water*.
- Suppasri, A., Koshimura, S., and Imamura, F. (2011). Developing tsunami fragility curves based on the satellite remote sensing and the numerical modeling of the 2004 Indian Ocean

- tsunami in Thailand. *Natural Hazards and Earth System Science*, 11(1):173–189.
- Suppasri, A., Mas, E., Charvet, I., Gunasekera, R., Imai, K., Fukutani, Y., Abe, Y., and Imamura, F. (2013). Building damage characteristics based on surveyed data and fragility curves of the 2011 Great East Japan tsunami. *Natural Hazards*, 66(2):319–341.
- Wiebe, D. M. and Cox, D. T. (2014). Application of fragility curves to estimate building damage and economic loss at a community scale: A case study of Seaside, Oregon. *Natural Hazards*, 71(3):2043–2061.